ZnO nanowires grown on bulk ZnO coatings: mechanical response to deep cryogenic treatment

M. Cabibbo

ZnO nanowires are currently used in many application fields, such emission displays, dye-sensitized solar cells, gas sensors, nanomachines, to cite but few. Thermal stability is often a concern in terms of the mechanical response and, in particular, for the elasticity of the nanowires. Literature works focused to a certain degree, on the heating response of nanowires. Anyhow, no experimental data are nowadays available in literature on the low- and very low-temperature exposures. In the present study, deep-cryogenic treatment was performed on vertically aligned ZnO nanowires produced by metal organic chemical vapor deposition. The mechanical response of the nanowires was detected by nanoindentation tests. It was found that the Young's modulus, the critical buckling stress and strain of individual nanowires is not significantly influenced by the cryogenic exposure. Yet, the bulk base ZnO from which the nanowires are grown halved after the deep-cryogenic treatment.

Keywords: ZnO nanowires - ZnO coatings - Nano-structured coatings - Deep-cryogenic treatment

INTRODUCTION

Zinc oxide (ZnO) has drawn considerable interest becauseof its semiconducting and piezoelectric properties [1-3]. In particular, ZnO nanostructures have applications asfield-effect transistors [4], gas sensors [5], field-emission displays [6], and nano-electromechanical systems (NEMS) [7]. All of theseapplications require the knowledge and the ability to controlthe mechanical behavior of ZnO nanostructures. ZnO possesses one of the richest family of nanostructures [3,8].ZnO has some advantages over the other above mentioned nanostructures as it exhibits both semiconducting and piezoelectric properties, and it can be grown in a wide variety of geometrical configurations [9].

Due to the reported high elastic modulus and high aspect ratio, a further potential application of ZnO NWs is as tips for atomic force microscopy. It has also been shown that thesematerials are potential useful for nanoscale interconnects,active components of optical electronic devices andnano-electromechanical systems. For these reasons, it is importantto understand mechanical characteristics of the ZnONWs[1,9-15].

Marcello Cabibbo
Dipartimento di Ingegneria Industriale e Scienze Matematiche (DIISM),
Università Politecnica delle Marche,
Via Brecce Bianche, 60131 Ancona

Presently, there are many reports on themechanical properties of ZnO NWs [16-18]. Recent experimental findings [18] reportedmodels to determining the buckling of ZnO NWs under uniaxial compression, and proposed a new method to observe thecritical load, elastic modulus, and stress or strain of the NWs based on the Euler or Johnson buckling theory.

There are several techniques that have been developed for measuring the elastic properties of individualNW. The technique first introduced by Wong, Sheehan, Lieber [1] is based on quantifying the deflection of a single nanowireaffixed at one end with the other end left free to be deflected by an atomic force microscope tip. The NWs were laid in parallel to a solid substrate, and the elastic modulus was calculated from the force-deflection curve.Moreover, mechanicalproperties of ZnO and similarNWs have been extensively studiedby tensile loading, bending, and buckling [19].

The study of nanoindentation on a vertically aligned nanowires (VANW) forest reveals a process whereby NWs are consecutively bent during the penetration of the indent tip. Therefore, the resistance of a VANW forest to penetration is due to successive bending of NWs as the tiptouches theNWs. Using a micro-mechanical model of the indentation process, the effective bending stiffness of constituent NWs in the VANW array is then deduced from nanoindentation force-penetrationdepth curves (essentially using the

classical Oliver and Pharr approach, see [20] to cite but one) [21]. Furthermore, when the size of a material is reduced to the nanoscale, owing to the large surface-to-volume ratio, surface effects will play important roles in the nanostructures. The theory of surface elasticity proposed by Gurtinet al. [22] has been widely employed and developed to account for the surface effects on nanoscale elements. Different techniques have been used to grow ZnO NWs, such as laser ablation [23], chemical vapor deposition method, electro-deposition method, vapor phase transport [11-14], thermal evaporation using ZnO powders [15], low-temperature liquid-phase deposition [24], vapor–liquid–solid deposition [25], electrochemical decomposition, which is a less onerous technique used in industry [26], and metal organic chemical vapor deposition (MOCVD) [14,27,28].
In this research work, ZnO NWs were grown by MOCVD in a Si-(100) substrate. In this work, the influence of a deep cryogenic treatment on MOCVD ZnO NWs mechanical properties such Young's modulus and hardness was studied.

EXPERIMETAL DETAILS

A vertical chamber MOCVD systemwas employed for the catalyst-free synthesis of theZnO NWs. Si-(100) wafer was used as thesubstrate. High-purity diethyl zinc (purity >99.99%), and N2O (purity >99.99%) were used as zinc and oxygensources, respectively, and nitrogen as the carrier gas.The diethyl zinc was kept at room temperature. The basepressure of the reactor chamber was 105 Torr, the working pressure being 40 Torr.
The ZnO NWswere grown via a two-step process. First, a thinnucleation layer of ZnO was grown at a temperature of 400°C. Thence, ZnO NWs were grown on the annealed nucleationlayer at a temperature of 650°C and for a total duration of 30 min.
The elastic properties and hardness of the vertical aligned ZnO NWs were measured by an indentation method [21] in which a tip was pushed downward against the aligned NWs so that many NWs are in contact with the tip (at least 30 individual NWs). By measurement of the force-displacement curve, and the average number of NWs that were in contact with the tip, an average elastic modulus and hardness estimation of the NWs is possible. This method requires that the density of the NWs is high and all of the NWs have the same size and length. To obtain statistically reliable data, different regions of the ZnO NWs were tested at different tip loads. Thus more than 100 measurements were carried out and the data reported hereafter were averaged over all the processed load-unload curves. Raw data analysis was performed according to the Oliver and Pharr method (readers interested to have more details on this widely used method of data analysis are referred to [20,29] and actually to the many other literature papers on nanoindentation data analysis). According to the round robin experiment results reported in [29], a trapezoid load function (loading time of 20 s, holding at the peak load for 60 s, followed by 3 s unloading to the 10% of the peak load, and a final 60 s holding at this load).
The Si/ZnO NWs samples were subjected to a cryogenic treatment consisting of a cooling from room temperature to -196°C at a rate of 1°C/min, holding at -196°c for 120 min, and slow recover to room temperature at same rate used for the cooling process.
A Hysitron©Inc. triboscope nanoindenterUbi®-1 was used to determine the Young's modulus and hardness of the ZnO NWs prior and after a cryogenic treatment. A uniaxial compression onto the ZnO NWswas exerted by a 3-sided pyramidal Berkovich tip (with edge aperture angle of 65.35°, and radius of curvature of 150 nm).
Samples surface morphology and size distribution of the NWs before andafter the cryogenic treatment and the nanoindentation tests were characterized by a Zeiss© Supra®-40 field emission scanning electron microscope(FESEM), operated at 5 KeV.

EXPERIMENTAL RESULTS AND DISCUSSION

Fig. 1 shows a cross-section FESEM image recorded at a 30° tilt angle of the as-grown ZnO NWs. It can be seenthat ZnO NWs are densely well-aligned with uniform diameter. Mean diameter, length and density of these NWs were 80 ± 5 nm, 1000 ± 80 nm, and $7.15 \cdot 10^9$ cm^{-2}, respectively. As shown in the Figure 1 inset, ZnO NWs were grown with an hexagonal structure.

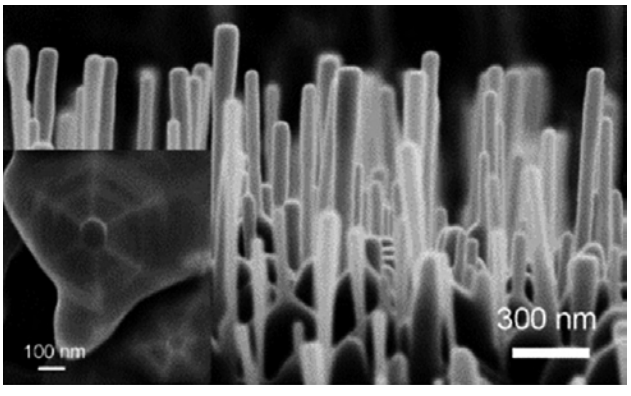

Fig. 1 - Cross-section FESEM image recorded at a 30° tilt angle showing diameter, length, and distribution of the as-grown ZnO NWs. Inset is a top-view showing the grown structure of the present ZnO NWs, which are hexagonal.

Fig. 2 reports a top-view FESEM micrograph of the deep-cryogenic treated NWs after nanoindentation test. It can be seen that these NWs were severely distorted and collapsed to the basement layer. Since these tests were destructive, several tests were carried out at different loads and in different ZnO NWs regions to ascertain the reproducible of the method. Results yield a full and reliable reproducibility of the method.

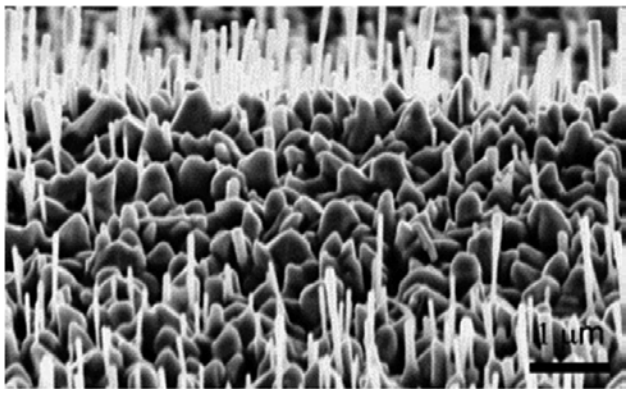

Fig. 2 - FESEM top-view of the deep-cryogenic treated ZnO NWs after a nanoindentation test (applied load of 7 mN, triangular pyramidal Berkovich tip).

A typical continuous load–unload force–displacement curve for as-grown and cryogenic treated NWs is shown in Figure 3. This figure clearly illustrates that multiple discontinuities, i.e. pop-in events, in the force–displacement curves occur during loading, in both cases, the as-grown NWs (Fig. 3(a)), and the deep-cryogenic treated condition (Fig. 3(b)). No discontinuities have been observed on unloading. Results show that the critical load for the first pop-in, that is the elastic-plastic threshold value, essentially varies in the range of 300-480 µN, in both conditions. More specifically, the as-growth NWs showed a average elastic-plastic threshold load value of 390 µN, and after cryogenic treatment this mean value was of 410 µN, that is, the mean critical load did not changed significantly after cryogenic treatment. In either cases, varying the applied load (in the range of 1 to 3.5 mN) the analysis of nanoindentation curves also revealed that the larger the load required for the first pop-in to occur, the larger the length of indenter excursion during the pop-in event, i.e. larger penetration depth. As a result, the maximum penetration of the indenter is essentially independent of the number of pop-in events during loading.

The loading portion of the load-displacement curves consist of three stages which can be recognized by the value of the critical load, Pcr: an initial load regime, where the load, P, increases (P < Pcr), followed by a sudden drop in the curve slope, which eventually becomes flat at P = Pcr, and a third stage,where the load starts back to increase with the penetration depth, P > Pcr. The buckling instability occurs in the flat portion of the loading curve. It is well known that the behavior of an ideal column ofNWs compressed by an axial load P can be summarized as follows: a. if P < Pcr, the column is in stable equilibrium in its straight position; b. if P = Pcr, the column is in a neutral equilibrium in either the straight or a slightly bent position; c. if P > Pcr, the column is in unstableequilibrium in its straight position and will buckle under the applied load.Such a type of buckling is called Euler buckling [30].

Fig. 3 also shows large displacement versus load in the load range P<Pcr, which denotes a large flexibility of the ZnO NWs. This behavior was observed not only in the as-grown condition, but also, and surprisingly, after deep-cryogenic treatment.In particular, the value of the critical load, Pcr, is essentially the same in either the as-grown and cryogenic treated condition, this ranges from 300 to 480 µN, in the as-grown NWs, and from 360 to 440 µN, in the cryogenic treated condition. An interesting aspect is thus that the range of variability of the buckling critical load after cryogenic treatment is far more narrow, and limited to the upper value portion of the value range showed in the as-grown condition. The ranging values of the ZnO NWs critical load depend on the applied maximum load, and in most cases it rises with applied load, which ranged 1.0 to 3.5 mN. Moreover, the penetration depth reached to initia-

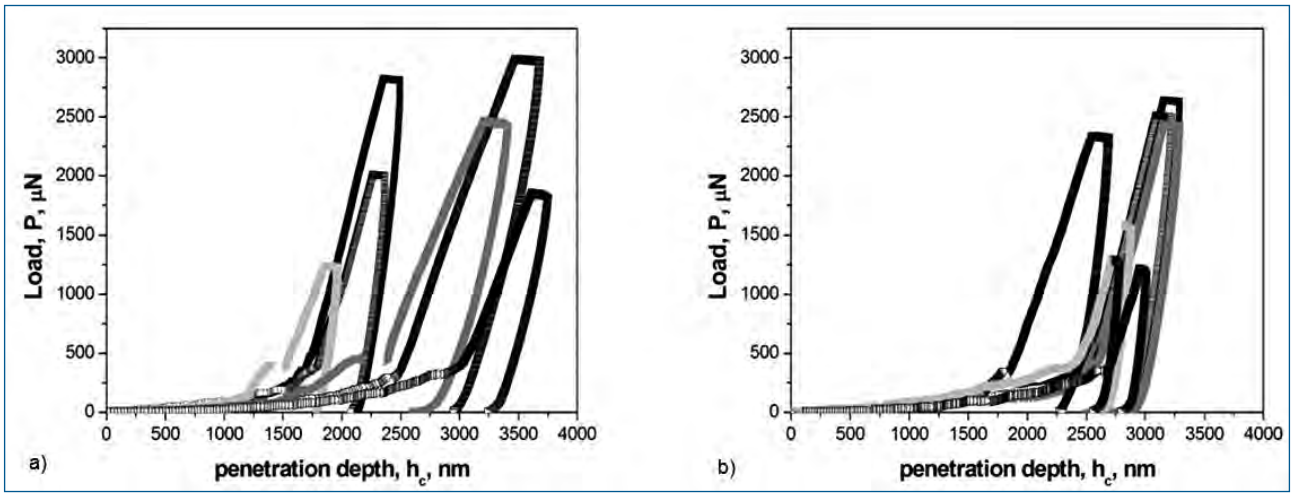

Fig. 3 - Six representative load-displacement nanoindentation curves showing the pop-in event upon loading of the ZnO NWs in the as-grown condition (maximum loads ranging1.25- to - 3.0 mN), a), and after deep-cryogenic treatment (cooling to -196 °C at a rate of 1 °C/min, holding at -196 °c for 120 min, followed by 1 °C/min slow recover to room temperature), where maximum loads ranged1.25-to-2.7 mN, b).

te the critical buckling load in the cryogenic treated ZnO NWs was the same as to the as-grown ZnO NWs. It is well known that the high flexibility of the ZnO NWs is attributed to the low dimension of the structure. For instance, Chen et al. [10] showed that a pure single ZnO crystal of 100 nm diameter can be bent into a minimum of 1 μm diameter circle. Another reason may be due to the movement of the NWs at the ends support, as a perfect rigid support is impossible, which is thus not influenced by the cryogenic treatment.

The FESEM top-view, reported in Fig. 2, easily allows the estimation of the average critical buckling load of an individual ZnO NW. As reported in Fig. 2, the area interacting with the indentation pyramidal tip is constituted by a equilateral triangle of 2 μm edge dimension (for typical applied loads of 2.5-3.5 mN), which slightly reduces to 1.7-1.8 μm in the lower load range (1.5-to-2.5 mN). The total ZnO NWs run over by the pyramidal tip are some 80. Thereafter, the critical buckling load of a single ZnO NW is about 4.9 and 5.1 μN, in the as-grown and cryogenic treated conditions, respectively. The unchanged buckling load of ZnO NWs after deep-cryogenic treatment is surely a remarkable result. This means that no change in the elastic-plastic properties of the ZnO NWs is induced by a cryogenic treatment.

Following the classical theory of elasticity of solids [33], the critical buckling load for an ideal elastic column can be expressed as (Euler load), Eq. (1):

$$P_{cr} = \pi 2EI/L_{eff}^{2} \quad (1)$$

where E is the Young's modulus of an individual ZnO NW, $I = \pi D^4/32$ is the momentum of inertia, D the mean NW diameter (this taken as the outer circumference of the NW hexagonal section), Leff is the effective NW length, which, for a fixed-pinned "cylindrical" NW is 0.7L, L being the mean NW length. The critical buckling strain is given by $\varepsilon cr = \sigma cr/E$, where the critical buckling stress, $\sigma cr = Pcr/A$, A being the mean section area of the hexagonal NWs $(A = (3\sqrt{3}/8)D^2)$.

Table 1 compiles the values obtained for the single ZnO NW Young's modulus, E, its critical buckling stress, σcr, and strain, εcr, in the as-grown and deep-cryogenic treated conditions. The quite close Young's modulus values (86 GPa for the as-grown, and 90 GPa of the deep-cryogenic treated single ZnO NW), accounting for a slight 4% difference, clearly indicate a almost irrelevant influence of the cryogenic treatment in the elastic modulus of the ZnO NWs.

The here obtained values are reasonably close to the reported elastic modulus of single-crystal ZnO bulk coating, being$E$ = 111 GPa as shown in [34]. The elastic properties of ZnO nanostructures and their size dependence have been previously investigated by means of transmission electron microscopy (TEM) [10] and atomic force microscopy (AFM) [30]. The Young's modulus of ZnO NWs was found to decrease dramatically with increasing diameter, reaching the

	P_{cr}, μN	E, GPa	σcr, MPa	εcr	variation, %
as-grown	4.9	86	1192	0.014	-
deep-cryogenic treated	5.1	90	1241	0.014	4

Table 1. Single ZnO NW critical buckling load, P_{cr}, Young's modulus, E, stress, σcr, and strain, εcr, in the as-grown and deep-cryogenic treated conditions.

ZnO bulk value for diameters typically larger than 120 nm. This behavior was attributed to a surface stiffening effect dominating at large surface-to-volume ratios [10].

The similar critical buckling stress in both conditions also means that hardness of individual ZnO NWs is not significantly modified after cryogenic treatment.

On the other hand, Oliver and Pharr analysis of the whole load-unload curves allowed to determine the Young's modulus and hardness of the ZnO NWs prior and after deep-cryogenic treatment. Anyhow, it must be emphasized that the classical Oliver and Pharr analysis approach of the raw data allows to determine the Young's modulus and hardness of the ZnO NWs, together with the basement from which they are grown. This is due to the fact that the third part of the loading curve, i.e. for $P > Pcr$, pertain to the ZnO coating basement, since the NW buckling load has been exceeded. Due to the fact that the Oliver and Pharr analysis determination of the coating Young's modulus and hardness are determined from the slope, i.e. the tangent, at the starting point of the unloading curve, the obtained value derives from both ZnO base and NWs. This holds unless the substrate of Si-(100) start to contribute to the measurements. This typically holds for penetration depths approaching 20-25% of the total coating thickness. In the present case, even the maximum applied load of 3.5 mN did not reach this limit (the penetration depth being of 3500 nm, under a ZnO base thickness of 20μm and NW of 1 μm).

Curve analysis showed that the as-grown NWs Young's modulus is $E_{as\text{-}grown}$, of 115 ± 25 GPa, which essentially doubled after deep-cryogenic treatment ($E_{post\text{-}cryo}$ = 320 ± 10 GPa). On the other hand, hardness increased slightly in the deep-cryogenic treated condition, being $H_{as\text{-}grown}$ = 4.4 ± 0.4 GPa, and $H_{post\text{-}cryo}$ = 5.3 ± 0.3 GPa. Elastic modulus and hardness of the base bulk ZnO coating well agreed with literature data (see for instance [35]).Thence, the hardness-to-elastic modulus ratio, H/E, of the ZnO coating, constituted by the base and NWs, almost halved after cryogenic treatment. Since, as shown above, the ZnO individual stress and Young's modulus did increase of only 4% after deep-cryogenic treatment, the larger part of reduction of the Young's modulus as determined by the load-unload curve analysis is to be attributed to the bulk base ZnO coating. This indeed is an interesting result, as it was shown that, while the elastic modulus of the ZnO bulk co-

ating halved after deep-cryogenic treatment, the ZnO NWs were practically not affected.

CONCLUSIONS

In summary, it was reported that deep-cryogenic treatment of MOCVD ZnO NWs did not impair the large flexibility of the as-grown ZnO NWs. It also did not influence to a significant extent the Young's modulus and the critical buckling load, stress , and strain. On the other hand, the Young's modulus of the bulk ZnO base, from which the NWs were grown, halved after the deep-cryogenic treatment.

ACKNOWLEDGMENTS

The authors wish to thank Mr. D. Ciccarelli for their help in performing the cryogenic treatment and nanoindentation tests.

RIFERIMENTI BIBLIOGRAFICI

[1] Z.L. WANG,J.H. SONG, Science 312 (2006) 242.
[2] M.-H. ZHAO,Z.L. WANG, S.X. MAO, Nano Lett. 4 (2004) 587.
[3] Z.L. WANG, J. Phys. Condens. Matter 16 (2004) R829.
[4] X. WANG,J. ZHOU,J. SONG, J. LIU,N. XU,Z.L. WANG, Nano Lett. 6 (2006) 2768.
[5] M.S. ARNOLD, P. AVOURIS, Z.W. PAN, Z. WANG, J. Phys. Chem. B 107 (2003) 659.
[6] C.J. LEE, T.J. LEE, S.C. LYU, Y.ZHANG, H. RUH, H. LEE, J. Appl. Phys. Lett. 81 (2002) 3648.
[7] W.L. HUGHES, Z.L. WANG, Appl. Phys. Lett. 82 (2003) 2886.
[8] A. DJURISIC, A. NG, X. CHEN, Prog. Quantum Electron. 34 (2010) 191.
[9] H. ZHOU, M. WISSINGER, J. FALLERT, R. HAUSCHILD, F.STELZL, C. KINGSHIRN, H. KALT, Appl. Phys. Lett. 91 (2007) 181112.
[10] C.Q. CHEN, Y. SHI, Y.S. ZHANG, J. ZHU, Y.J. YAN, Phys. Rev. Lett. 96 (2006) 075505.
[11] D.C. LOOK, Mater. Sci. Eng. B 80 (2001) 383.
[12] S. MUTHUKUMAR, H. SHEN, J. ZHONG, Z. ZHANG, N.W. EMANTOGLU, Y. LU, IEEE Trans. Nanotechnol. 2 (2003) 50.
[13] W. LEE, M.C. JEONG, J.M. MYOUNG, Acta Mater. 52 (2004) 3949.
[14] Z.R. DAI, Z.W. PAN, Z.L. WANG, Adv. Funct. Mater. 13 (2003) 9.
[15] Z.W. PAN, Z.R. DAI, Z.L. WANG, Science 291 (2010) 1947.
[16] C.Q. CHEN, J. ZHU, Appl. Phys. Lett. 90 (2007) 043105.
[17] S.J. YOUNG, L.W. LI, S.J. CHANG, T.H. FANG, T.J. HSUEH, T.H. MEEN, I.C. CHEN, Nanotechnology 18 (2007) 225603.
[18] M. RIAZ, O. NUR, M. WILLANDER, P. KLASON, Appl. Phys. Lett. 92 (2008) 103118.
[19] M.F. YU, O. LOURIE, M.J. DYER, K. MOLONI, T.F. KELLY, R.S. RUOFF, Science 287 (2000) 637.
[20] W.C. OLIVER, G.M. PHARR, J. Mater. Res. 7 (1992) 1564.
[21] H.J. QI, K.B.K. TEO, K.K.S. LAU, M.C. BOYCE, W.I. MILNE, J. ROBERTSON, K.K. GLEASON, J. Mech. Phys. Solids 51 (2003) 2213.
[22] M.E. GURTIN, J. WEISSMULLER, F. LARCHE', Phil. Mag. A 78 (1998) 1093.
[23] B.M. ATAEV, I.K. KAMILOV, V.V. MAMEDOV, ,Tech. Phys. Lett. 23 (1997) 842.
[24] F. XU, Z.Y. YUAN, G.H. DU, T.Z. REN, C. VOLCKE, P. THIRY, B.L. SU, J. Non-Crystal. Solids 352 (2006) 2569.
[25] Y.S. ZHANG, K. YU, S.X. OUYANG, Z.Q. ZHU, Mater. Lett. 60 (2006) 522.
[26] Y. LEPRINCE-WANG, G.Y. WANG, X.Z. ZHANG, D.P. YU, J. Crystal Growth 287 (2006) 89.
[27] J.Y. PARK, D.J. LEE, Y.S. YUN, J.H. MOON, B.T.LEE, S.S. KIN, J. Crystal Growth 276 (2005) 158.
[28] Y.J. ZENG, Z.Z YE, W.Z. XU, L.P. ZHU, B.H. ZHAO, Appl. Surf. Sci. 250 (2005) 280.
[29] M. CABIBBO, P. RICCI, R.CECCHINI, Z. RYMUZA, J. SULLIVAN, S. DUB, S. COHEN, Micron 43 (2012) 215.
[30] W.J. MAI, Z.L. WANG, Appl. Phys. Lett. 89 (2006) 073112.
[31] L.W. JI, S.J. YOUNG, T.H. FANG, C.H. LIU, Appl. Phys. Lett. 90 (2007) 033109.
[32] S.J. YOUNG, L.W. JI, S.J. CHANG, T.H.FANG, T.J. HSUEH, Physica E 39 (2007) 240.
[33] S.P. TIMOSHENKO, J.M.GERE, Theory of Elastic Stability McGraw-Hill, New York, 1961, p. 46.
[34] S.O. KUCHEYEV, J.E. BRADBY, J.S. WILLIAMS, C. JAGADISH, M.V.SWAIN, Appl. Phys. Lett. 80 (2002) 956.